symmetry

MDPI

Article

Bilateral Correlational Behavior of Pyroglutamate Aminopeptidase I Activity in Rat Photoneuroendocrine Locations During a Standard 12:12 h Light–Dark Cycle

Manuel Ramírez-Sánchez [1,*], Isabel Prieto [1], Ana Belén Segarra [1], Inmaculada Banegas [1], Magdalena Martínez-Cañamero [1], Germán Domínguez-Vías [2], Raquel Durán [3] and Francisco Vives [3]

[1] Department of Health Sciences, University of Jaén, 23071 Jaén, Spain; iprieto@ujaen.es (I.P.); asegarra@ujaen.es (A.B.S.); ibanegas@ujaen.es (I.B.); canamero@ujaen.es (M.M.-C.)
[2] Department of Physiology, Faculty of Health Sciences, Ceuta, University of Granada, 18071 Granada, Spain; germandv@go.ugr.es
[3] Department of Physiology, Faculty of Medicine, University of Granada, 18071 Granada, Spain; rduran@ugr.es (R.D.); fvives@ugr.es (F.V.)
* Correspondence: msanchez@ujaen.es

Abstract: We previously described the circadian variation and bilateral distribution of pyroglutamate aminopeptidase I (pGluPI) activity levels in photoneuroendocrine locations of adult male rats during a standard 12:12 h light–dark cycle. However, the correlational analysis between such locations has not yet been studied. This may provide new data about the unilateral and bilateral functional interaction between photoneuroendocrine locations under light and dark conditions. We analyzed the correlations between locations of a photoneuroendocrine circuit consisting of retina, anterior hypothalamus, superior cervical ganglion, and pineal gland, as well as other related photoneuroendocrine locations: posterior hypothalamus, anterior pituitary, posterior pituitary, occipital cortex, and serum. In particular, we analyzed the correlations between the left retina or the right retina versus the rest of the locations, as well as the correlations between the left and right sides of paired structures at the different time points selected from 12 h light and 12 h dark periods. Also, the profiles of correlational results were compared with the corresponding mean levels. The results demonstrate the complexity of asymmetrical brain behavior. The correlation profile did not always parallel the profile observed with the mean activity values. The diurnal behavior of correlations with the left or right retina differed from one location to another. Likewise, the diurnal variation of correlations between the left and right sides of the paired structures differed between them. Particularly, while most correlations between the left versus right sides of paired structures showed positive values, that of the posterior hypothalamus showed a negative value at 13 h of light period. In addition, except the posterior hypothalamus, most paired locations only correlated significantly with right retina at 07 h of the light period. The results demonstrate the dynamic complexity of brain asymmetry, which represents a challenge for understanding its functional meaning.

Keywords: brain asymmetry; intra-hemispheric correlations; inter-hemispheric correlations; photoneuroendocrine locations

Citation: Ramírez-Sánchez, M.; Prieto, I.; Segarra, A.B.; Banegas, I.; Martínez-Cañamero, M.; Domínguez-Vías, G.; Durán, R.; Vives, F. Bilateral Correlational Behavior of Pyroglutamate Aminopeptidase I Activity in Rat Photoneuroendocrine Locations During a Standard 12:12 h Light–Dark Cycle. *Symmetry* **2024**, *16*, 1539. https://doi.org/10.3390/sym16111539

Academic Editor: John H. Graham

Received: 12 October 2024
Revised: 12 November 2024
Accepted: 15 November 2024
Published: 17 November 2024

1. Introduction

Pyroglutamate aminopeptidase I (pGluPI) is a proteolytic enzyme involved in, among other functions, the metabolism of thyrotropin releasing hormone (TRH) and gonadotropin releasing hormone (GnRH), both acting as neurotransmitters or neurohormones [1,2]. The N-terminal pyroglutamic residue of these neuropeptides is hydrolyzed by pGluPI (EC 3.4.19.3). This enzyme has been found in soluble and particulate fractions of tissues [1]. However, the results obtained by Alba et al. [3] suggest that the soluble and

membrane-bound forms of the enzyme represent the same protein in two different subcellular compartments. In addition, pGluPI has been proposed to be useful for the diagnosis and treatment of inflammation [4]. Previously, in adult male rats [5], the variation of pGluPI activity levels was described at several time points in a 12:12 h light (resting)–dark (active) cycle, in paired and unpaired locations within a photoneuroendocrine circuit formed by the retina, anterior hypothalamus, superior cervical ganglion, and pineal gland [6,7] as well as in other related locations such as the posterior hypothalamus, anterior pituitary, posterior pituitary, occipital cortex, and serum [8–10]. The circuit was closed by pinealocyte projections [7] and melatonin receptors in brain locations such as the suprachiasmatic or arcuate nuclei [11] and also in the retina, which is itself capable of synthesizing melatonin via its photoreceptors [12]. However, the correlational analysis between such locations, necessary in the context of brain asymmetry, has not yet been studied and may offer a new different point of view regarding the investigation of the mean levels. This analysis may provide new data about the unilateral and bilateral functional interaction between photoneuroendocrine locations under conditions of light and darkness. We analyzed the correlation of pGluPI activity between the photoneuroendocrine locations: retina, anterior hypothalamus, superior cervical ganglion, pineal gland, posterior hypothalamus, anterior pituitary, posterior pituitary, occipital cortex, and serum, at several time points selected from the 12 h light and 12 h dark periods. (Figure 1). In particular, we analyzed the correlations between the left retina and the right retina versus the rest of the locations, as well as the correlations between the left and right sides of the paired structures at the different time points selected from the 12 h light and 12 h dark periods (Figure 2). Also, the profiles of correlational results were compared with the corresponding mean levels. In order to analyze pGluPI activity, pyroglutamyl-beta-naphthylamide (L-pGluNNap) was used as substrate [13].

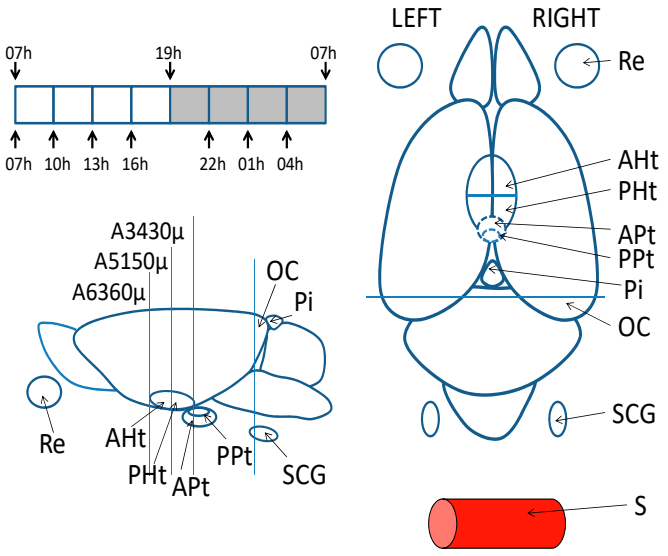

Figure 1. Indicative scheme of the artificial regime of 12 h light and 12 h darkness (light from 07 h to 19 h, darkness from 19 h to 07 h) to which the animals were subjected. The arrows indicate the times at which the areas to be analyzed were obtained (07 h, 10 h, 13 h, 16 h in light conditions; 22 h, 01 h, 04 h in dark conditions). Dorsal and lateral views of the rat brain are also schematically represented. They indicate the locations in which pGluPI activity was determined: retina (Re), anterior (AHt) and posterior hypothalamus (PHt), anterior (APt) and posterior (PPt) pituitary gland, pineal gland (Pi), occipital cortex (OC), superior cervical ganglion (SCG), and serum (S). The lateral view indicates the levels anterior to the interatrial line between which coronal sections were made to obtain AHt and PHt [14]. OC was obtained from a coronal section of the most caudal part of the occipital lobe.

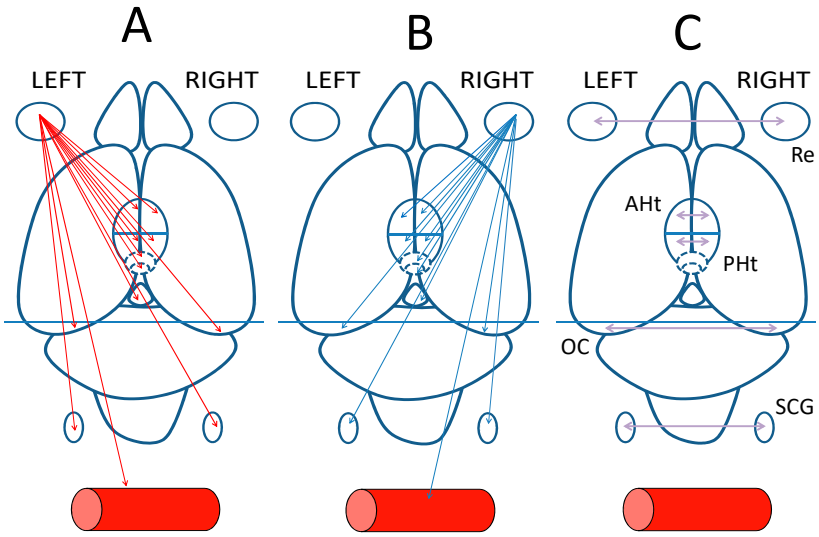

Figure 2. Correlations analyzed in the present work: (**A**) between the left retina and the rest of the locations (red arrows); (**B**) between the right retina and the rest of the locations (blue arrows); (**C**) between the left and right sides of paired locations (purple arrows).

2. Material and Methods

For this study, male Sprague–Dawley rats with an average weight of 225 g were used. The experiments were carried out in accordance with the ethical parameters approved by the European Communities Council Directive 86/609/EEC. Until the time of the surgical procedure, the animals were kept at a constant temperature (25 °C), with food and water ad libitum, under a regime of 12 h light, 12 h darkness. The light period lasted from 07 h to 19 h and the dark period lasted from 19 h to 07 h. The procedure for obtaining tissue samples began at 07 h, 10 h, 13 h, and 16 h of the light period and at 22 h, 01 h, and 04 h of the dark period (Figure 1). The experimental sequence is schematized in Figure 3 and was as detailed previously [13]. Briefly, animals were anesthetized intraperitoneally with equitensin (0.2 mL/100 g of body weight). Prior to the perfusion of the animal with physiological saline (0.9% NaCl), blood samples were obtained via the left ventricle and serum (S) samples were collected. During the dark hours, the animals were perfused under red light and white light was used only once the eyeballs were removed. After perfusion and prior to the brain extraction, the eyes were obtained and their left (ReL) and right (ReR) retinas were dissected. The left (SCGL) and right (SCGR) superior cervical ganglia were also obtained. The brains were then extracted and at the same time, the pineal gland (Pi) and pituitary gland were dissected, the latter being separated into its anterior (APt) and posterior (PPt) portions. The brain was sectioned in a rostrum–caudal coronal manner according to the stereotaxic atlas of König and Klippel [14]. The left anterior hypothalamus (AHtL) and right anterior hypothalamus (AHtR), the left posterior hypothalamus (PHtL) and right posterior hypothalamus (PHtR), the most caudal portion of the occipital lobe, the left occipital cortex (OCL), and the right occipital cortex (OCR) were dissected. The anterior hypothalamic area was considered to be the brain tissue between the stereotaxic planes A6360 µ and A5150 µ anterior to the interatrial line (containing the anterior hypothalamic, suprachiasmatic, and paraventricular nuclei, among others). The posterior hypothalamic area was considered to be between the planes A5150 µ and A3430 µ (containing the dorsomedial, ventromedial, and arcuate nuclei, among others). Once the tissue samples were obtained, they were homogenized and ultracentrifuged to obtain the supernatant used for the determination of pGluPI and proteins. The activity of pGluPI was determined fluorimetrically using pGluNNap as substrate [13]. The amount of protein was determined according to the Bradford method [15]. The activity of pGluPI was expressed as pmol of pGluNNap hydrolyzed per min and per mg of proteins.

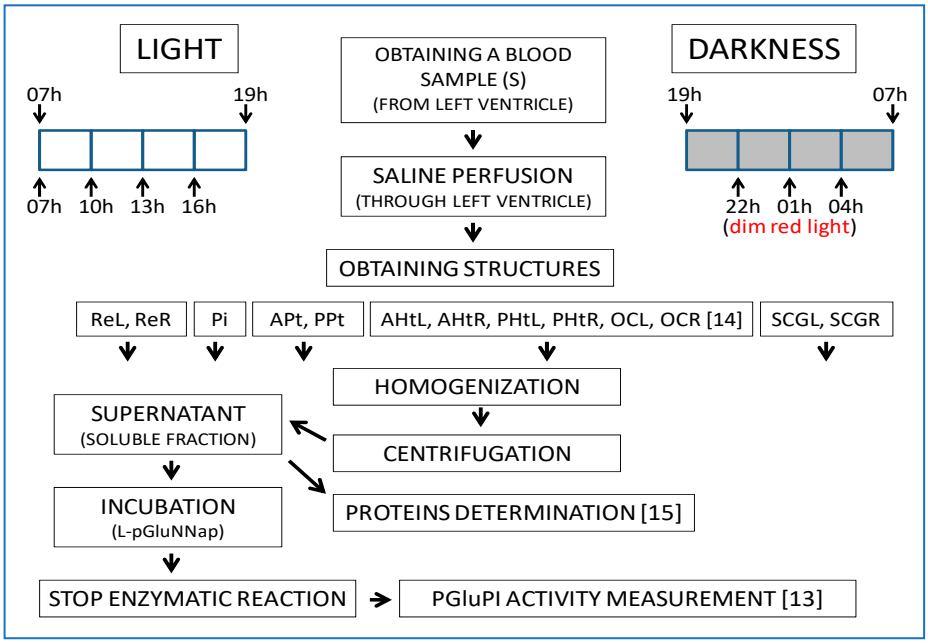

Figure 3. Diagram showing the experimental sequence for obtaining samples and determining enzymatic activity under light or dark conditions [5]. Briefly, after anesthetizing the animal, a blood sample was obtained from the left ventricle. The rat brain was then perfused with isotonic saline solution and the areas of interest were dissected and processed. The soluble fraction was isolated and the enzymatic activity and protein quantity were determined. Brain structures were obtained via coronal section according to the König and Klippel atlas [14] (Figure 1). Abbreviations: AHtL, left anterior hypothalamus, AHtR, right anterior hypothalamus, APt, anterior pituitary, L-pGluNNap, pyroglutamyl-beta-naphthylamide, OCL, left occipital cortex, OCR, right occipital cortex, PGluPI, pyroglutamyl peptidase I, PHtL, left posterior hypothalamus, PHtR, right posterior hypothalamus, Pi, pineal gland, PPt, posterior pituitary, ReL, left retina, ReR, right retina, SCGL, left superior cervical ganglion, SCGR, right superior cervical ganglion.

Using such data, whose mean values were previously published [5], we carried out correlational analysis between the left (ReL) or right (ReR) retinas versus the rest of the obtained zones, at each of the selected time points during the light and dark periods (Figures 1 and 2). We also obtained the correlation levels between the left and right sides of the paired zones (Re, AHt, PHt, OC, SCG) at each of the time points under light and dark conditions (Figure 2). We also compared the correlational profiles with the ones obtained using the mean values. Pearson's coefficients of correlation were used to calculate the levels of correlation between Re and the rest of the locations, as well as between the left and right sides of the paired zones. The calculations were carried out using SPSS 13.0 and STATA 9.0 (STATA Corp, College Station, TX, USA).

3. Results

The correlation and significance levels between the left (ReL) or right retinas (ReR) and all the analyzed structures are shown in Table 1 and represented in Figures 4–8. Those between the left and the right sides of paired structures are shown in Table 2 and represented in Figure 9. Figure 10 specifically represents the correlations between the left or right retina and the left or right posterior hypothalamus.

Table 1. Levels of correlation (*r*) and significance (*p*) between the left (ReL) or right retinas (ReR) and all the analyzed structures (APt, PPt, AHtL, AHtR, PHtL, PHtR, SCGL, SCGR, OCL, OCR, Pi, S) in selected time points of the light (07 h, 10 h, 13 h, 16 h) and dark periods (22 h, 01 h, 04 h). Significant correlations highlighted in bold and cursive. Negative correlations in red. Number of animals in parenthesis. These results are represented in Figures 4–8.

ReL and ReR vs. Rest Diurnal														
	ReL	**ReR**	**APt**	**PPt**	**AHtL**	**AHtR**	**PHtL**	**PHtR**	**SCGL**	**SCGR**	**OCL**	**OCR**	**Pi**	**S**
ReL 07 h (n = 11)	1	*r* 0.241 *p* 0.475	*r* 0.598 *p* 0.052	*r* 0.609 *p* 0.046	*r* 0.413 *p* 0.206	*r* 0.380 *p* 0.249	*r* 0.608 *p* 0.047	*r* 0.541 *p* 0.085	*r* 0.521 *p* 0.100	*r* 0.475 *p* 0.139	*r* 0.461 *p* 0.153	*r* 0.339 *p* 0.307	*r* 0.464 *p* 0.150	*r* 0.394 *p* 0.230
ReR 07 h (n = 11)	*r* 0.241 *p* 0.475	1	*r* 0.747 *p* 0.008	*r* 0.668 *p* 0.024	*r* 0.609 *p* 0.046	*r* 0.630 *p* 0.037	*r* 0.569 *p* 0.067	*r* 0.738 *p* 0.009	*r* 0.806 *p* 0.002	*r* 0.726 *p* 0.011	*r* 0.733 *p* 0.010	*r* 0.792 *p* 0.003	*r* 0.531 *p* 0.092	*r* 0.116 *p* 0.734
ReL 10 h (n = 8)	1	*r* 0.772 *p* 0.024	*r* 0.464 *p* 0.246	*r* 0.283 *p* 0.497	*r* 0.312 *p* 0.451	*r* 0.015 *p* 0.971	*r* 0.542 *p* 0.165	*r* 0.437 *p* 0.279	*r* 0.302 *p* 0.467	*r* 0.045 *p* 0.915	*r* 0.354 *p* 0.389	*r* 0.799 *p* 0.017	*r* 0.263 *p* 0.529	*r* 0.343 *p* 0.405
ReR 10 h (n = 8)	*r* 0.772 *p* 0.024	1	*r* 0.279 *p* 0.503	*r* 0.475 *p* 0.234	*r* 0.684 *p* 0.061	*r* 0.437 *p* 0.279	*r* 0.664 *p* 0.072	*r* 0.684 *p* 0.061	*r* 0.367 *p* 0.371	*r* 0.112 *p* 0.791	*r* 0.500 *p* 0.207	*r* 0.763 *p* 0.027	*r* 0.630 *p* 0.094	*r* 0.272 *p* 0.514
ReL 13 h (n = 6)	1	*r* 0.873 *p* 0.023	*r* 0.463 *p* 0.355	*r* 0.454 *p* 0.365	*r* 0.008 *p* 0.988	*r* 0.145 *p* 0.784	*r* 0.238 *p* 0.649	*r* −0.09 *p* 0.852	*r* 0.497 *p* 0.315	*r* 0.576 *p* 0.231	*r* 0.816 *p* 0.047	*r* 0.324 *p* 0.531	*r* 0.628 *p* 0.181	*r* 0.662 *p* 0.152
ReR 13 h (n = 6)	*r* 0.873 *p* 0.023	1	*r* 0.235 *p* 0.654	*r* 0.572 *p* 0.235	*r* 0.341 *p* 0.508	*r* 0.388 *p* 0.447	*r* 0.674 *p* 0.142	*r* −0.453 *p* 0.367	*r* 0.391 *p* 0.443	*r* 0.496 *p* 0.317	*r* 0.760 *p* 0.079	*r* 0.334 *p* 0.517	*r* 0.381 *p* 0.456	*r* 0.668 *p* 0.147
ReL 16 h (n = 6)	1	*r* 0.322 *p* 0.533	*r* −0.67 *p* 0.144	*r* 0.001 *p* 0.998	*r* 0.424 *p* 0.402	*r* 0.476 *p* 0.339	*r* 0.737 *p* 0.094	*r* 0.705 *p* 0.117	*r*−0.08 *p* 0.868	*r* 0.323 *p* 0.532	*r* −0.11 *p* 0.882	*r* 0.801 *p* 0.055	*r* −0.380 *p* 0.457	*r* −0.26 *p* 0.618
ReR 16 h (n = 6)	*r* 0.322 *p* 0.533	1	*r* −0.03 *p* 0.943	*r* 0.520 *p* 0.290	*r* 0.382 *p* 0.454	*r* 0.825 *p* 0.043	*r* 0.746 *p* 0.088	*r* 0.875 *p* 0.022	*r* 0.284 *p* 0.585	*r* 0.804 *p* 0.053	*r* 0.428 *p* 0.397	*r* 0.315 *p* 0.543	*r* 0.256 *p* 0.624	*r* 0.202 *p* 0.701
ReL 22 h (n = 6)	1	*r* 0.852 *p* 0.031	*r* 0.933 *p* 0.006	*r* 0.406 *p* 0.424	*r* −0.325 *p* 0.529	*r* −0.16 *p* 0.759	*r* 0.658 *p* 0.155	*r* 0.705 *p* 0.117	*r* 0.416 *p* 0.412	*r* 0.875 *p* 0.022	*r* 0.793 *p* 0.059	*r* 0.964 *p* 0.001	*r* 0.892 *p* 0.016	*r* −0.22 *p* 0.663
ReR 22 h (n = 6)	*r* 0.852 *p* 0.031	1	*r* 0.832 *p* 0.04	*r* 0.172 *p* 0.744	*r* −0.655 *p* 0.158	*r* −0.35 *p* 0.487	*r* 0.612 *p* 0.196	*r* 0.659 *p* 0.154	*r* 0.247 *p* 0.637	*r* 0.626 *p* 0.183	*r* 0.607 *p* 0.201	*r* 0.877 *p* 0.021	*r* 0.715 *p* 0.110	*r* −0.50 *p* 0.303
ReL 01 h (n = 8)	1	*r* 0.560 *p* 0.148	*r* 0.594 *p* 0.120	*r* 0.277 *p* 0.506	*r* −0.131 *p* 0.757	*r* −0.12 *p* 0.766	*r* −0.32 *p* 0.433	*r* −0.31 *p* 0.453	*r* 0.078 *p* 0.854	*r* 0.175 *p* 0.678	*r* 0.384 *p* 0.347	*r* 0.754 *p* 0.030	*r* −0.380 *p* 0.353	*r* 0.282 *p* 0.498
ReR 01 h (n = 8)	*r* 0.560 *p* 0.148		*r* 0.921 *p* 0.001	*r* 0.541 p 0.166	*r* −0.491 *p* 0.216	*r* −0.30 *p* 0.467	*r* −0.29 *p* 0.473	*r* −0.08 *p* 0.835	*r* 0.783 *p* 0.021	*r* 0.623 *p* 0.098	*r* 0.841 *p* 0.008	*r* 0.434 *p* 0.282	*r* 0.471 *p* 0.238	*r* 0.548 *p* 0.159
ReL 04 h (n = 8)	1	*r* 0.373 *p* 0.362	*r* 0.287 *p* 0.490	*r* 0.072 *p* 0.865	*r* −0.077 *p* 0.856	*r* −0.29 *p* 0.482	*r* −0.76 *p* 0.026	*r* −0.08 *p* 0.843	*r* 0.628 *p* 0.095	*r* 0.510 *p* 0.196	*r* 0.503 *p* 0.203	*r* 0.549 *p* 0.158	*r* 0.021 *p* 0.960	*r* 0.361 *p* 0.379
ReR 04 h (n = 8)	*r* 0.373 *p* 0.362	1	*r* 0.395 *p* 0.332	*r* −0.30 *p* 0.467	*r* −0.235 *p* 0.575	*r* −0.58 *p* 0.130	*r* 0.036 *p* 0.932	*r* −0.28 *p* 0.490	*r* 0.170 *p* 0.687	*r* 0.233 *p* 0.578	*r* 0.921 *p* 0.001	*r* 0.498 *p* 0.209	*r* 0.118 *p* 0.780	*r* 0.720 *p* 0.044

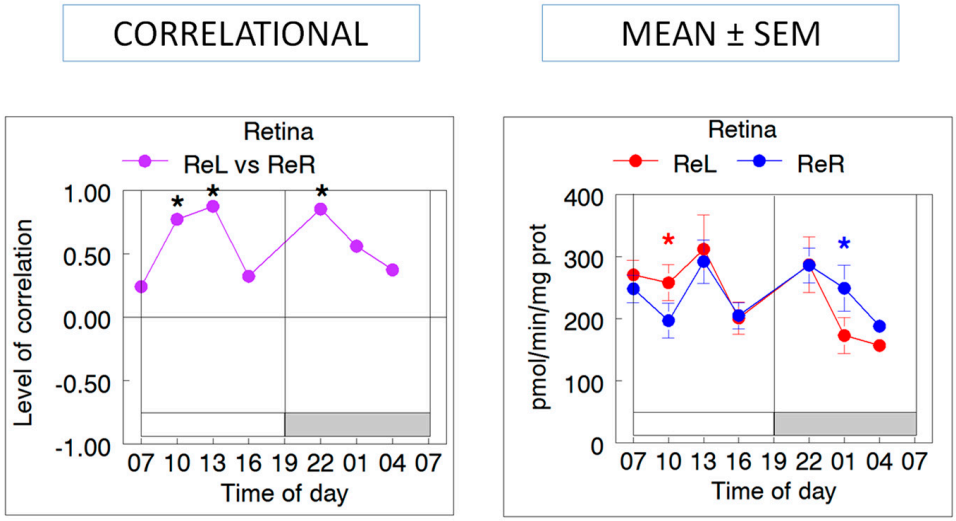

Figure 4. Representation of the profiles of correlational values between left (ReL) vs. right (ReR) retinas (* significant difference for this correlation) and mean ± SEM levels of ReL and ReR throughout the 12:12 h light–dark cycle (* significant left predominance, * significant right predominance).

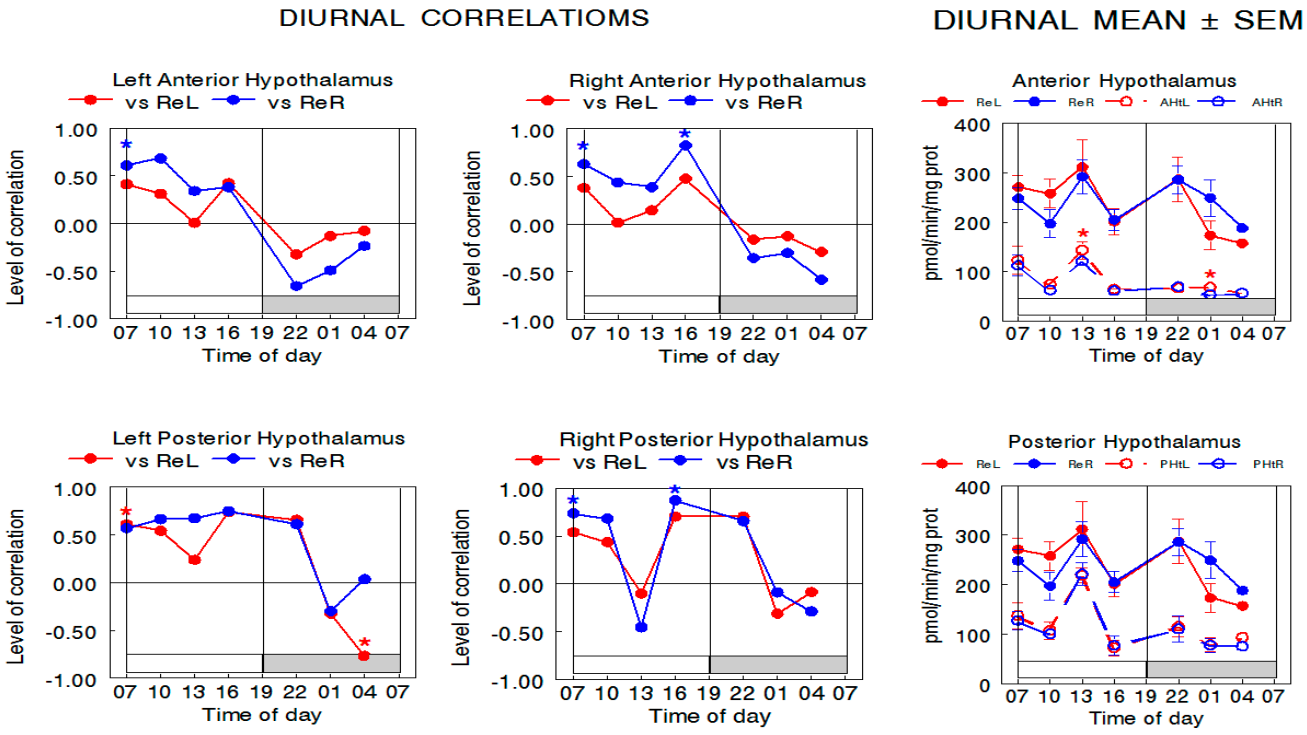

Figure 5. Representation of the profiles of correlational values between the left anterior hypothalamus, right anterior hypothalamus, left posterior hypothalamus, and right posterior hypothalamus, each versus the left (ReL) or right (ReR) retinas (* significant difference vs. ReR; * significant difference vs. ReL) and mean ± SEM levels of ReL and ReR throughout the 12:12 h light–dark cycle (continuous lines) in comparison with the mean ± SEM levels of left versus right anterior or posterior hypothalamus (discontinuous lines) (* significant left predominance).

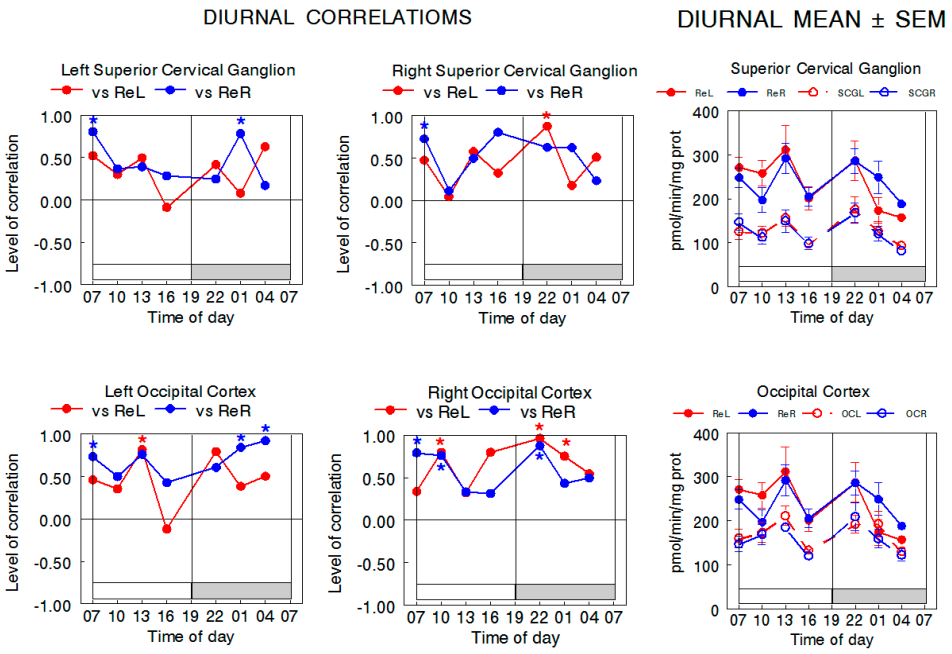

Figure 6. Representation of the profiles of correlational values between the left superior cervical ganglion, right superior cervical ganglion, left occipital cortex, and right occipital cortex, each one versus the left (ReL) or right (ReR) retinas (* significant difference vs. ReR; * significant difference vs. ReL) and mean ± SEM levels of ReL and ReR throughout the 12:12 h light–dark cycle (continuous lines) in comparison with the mean ± SEM levels of left versus right superior cervical ganglion and occipital cortex (discontinuous lines).

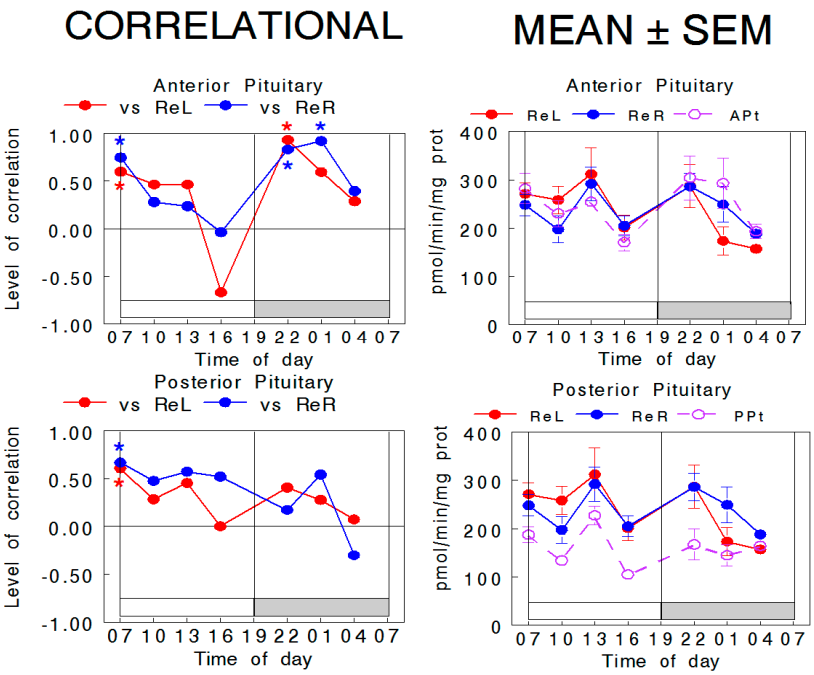

Figure 7. Representation of the profiles of correlational values between the anterior and posterior pituitary, each versus the left (ReL) or right (ReR) retinas (* significant difference vs. ReR; * significant difference vs. ReL) and mean ± SEM levels of ReL and ReR throughout the 12:12 h light–dark cycle (continuous lines) in comparison with the mean ± SEM levels of anterior and posterior pituitary (discontinuous lines).

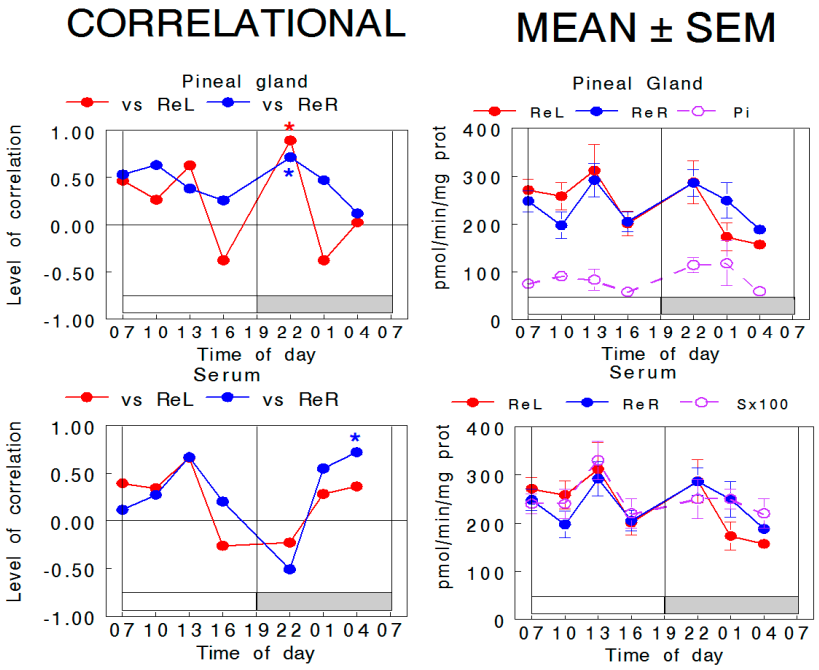

Figure 8. Representation of the profiles of correlational values between the pineal gland and serum, each versus left (ReL) or right (ReR) retinas (* significant difference vs. ReR; * significant difference vs. ReL) and mean ± SEM levels of ReL and ReR throughout the 12:12 h light–dark cycle (continuous lines) in comparison with the mean ± SEM levels of pineal gland and serum (values × 100) (discontinuous lines).

Table 2. Levels of correlation (*r*) and significance (*p*) between the left and right sides of paired structures (Re, AHt, PHt, SCG, OC) at the time points during the light and dark periods. Significant correlations highlighted in bold and cursive. Negative correlations in red. Number of animals in parenthesis. These results are represented in Figure 9.

	Left vs. Right Diurnal				
	Re	**AHt**	**PHt**	**SCG**	**OC**
07 h (n = 11)	*r* 0.241 *p* 0.475	*r* 0.930 *p* < 0.0001	*r* 0.929 *p* < 0.0001	*r* 0.924 *p* < 0.0001	*r* 0.934 *p* < 0.0001
10 h (n = 8)	*r* 0.772 *p* 0.024	*r* 0.678 *p* 0.064	*r* 0.801 *p* 0.016	*r* 0.697 *p* 0.054	*r* 0.710 *p* 0.048
13 h (n = 6)	*r* 0.873 *p* 0.023	*r* 0.967 *p* 0.001	*r* −0.820 *p* 0.045	*r* 0.900 *p* 0.014	*r* 0.662 *p* 0.152
16 h (n = 6)	*r* 0.322 *p* 0.533	*r* 0.804 *p* 0.053	*r* 0.948 *p* 0.004	*r* 0.626 *p* 0.183	*r* 0.287 *p* 0.581
22 h (n = 6)	*r* 0.852 *p* 0.031	*r* 0.772 *p* 0.072	*r* 0.981 *p*.0005	*r* 0.471 *p* 0.345	*r* 0.840 *p* 0.036
01 h (n = 8)	*r* 0.560 *p* 0.148	*r* 0.871 *p* 0.004	*r* 0.955 *p*.0002	*r* 0.766 *p* 0.026	*r* 0.601 *p* 0.115
04 h (n = 8)	*r* 0.373 *p* 0.362	*r* 0.358 *p* 0.383	*r* 0.467 *p* 0.243	*r* 0.712 *p* 0.047	*r* 0.474 *p* 0.235

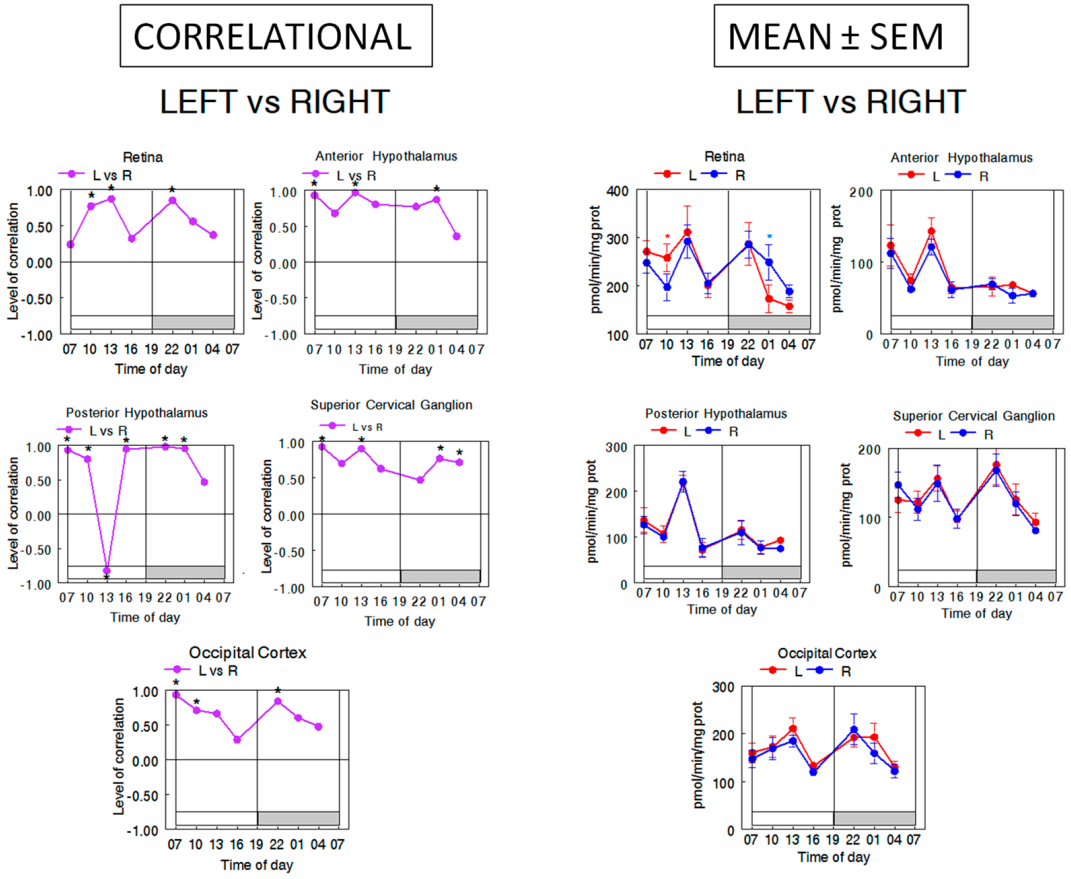

Figure 9. Representation of the profiles of correlational values between the left or right sides of paired structures: retina, anterior hypothalamus, posterior hypothalamus, superior cervical ganglion, and occipital cortex (* significant difference between left versus right side) and mean ± SEM levels of the same locations throughout the 12:12 h light–dark cycle (* significant left predominance, * significant right predominance).

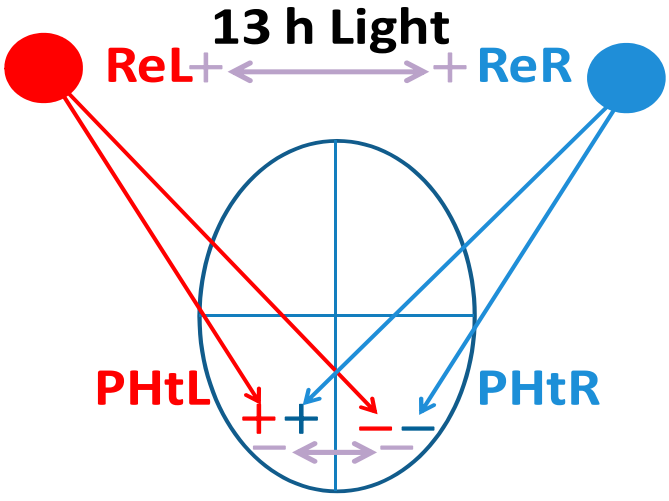

Figure 10. Positive (+) or negative (−) behavior of the correlations between the left retina (ReL) (red) and the right retina (ReR) (blue) versus the left posterior hypothalamus (PHtL) or the right posterior hypothalamus (PHtR) (Figure 5). The negative correlations between the PHtL and PHtR and the positive ones between the ReL and ReR at 13 h in the light period are also indicated (violet arrows) (Figure 9).

For comparative purposes, on the right side of Figures 4–8, the profiles of correlational values throughout the 12:12 h light–dark cycle are represented together with their corresponding mean ± SEM levels [5]. In Figures 5–8, also for comparative purposes, in each figure (mean ± SEM levels), along with the diurnal profiles of the left and right sides of each structure (dashed lines), the diurnal profiles of the left and right values of the retina (solid lines) are included.

The correlational analysis between the left and right retina showed significant positive levels at 10 h (r = +0.772, $p < 0.024$, n = 8), at 13 h (r = +0.873, p = 0.023, n = 6), and at 22 h (r = +0.852, $p < 0.031$, n = 6) (Figure 4).

The correlational analysis between the left anterior hypothalamus and the left or right retina demonstrated a significant positive value versus right retina only at 07 h (r = +0.609, p = 0.046, n = 11). The correlation between the left or right retina and the right anterior hypothalamus demonstrated positive significance versus the right retina at 07 h (r = +0.630, p = 0.037, n = 11) and also, positive significance versus the right retina at 16 h (r = +0.825, p = 0.043, n = 6). The left posterior hypothalamus correlated significantly positively with the left retina at 07 h (r = +0.608, p = 0.047, n = 11) and negatively with the left retina at 04 h (r = 0.767, p = 0.026, n = 8). The right posterior hypothalamus correlated significantly positively with the right retina at 07 h (r = +0.738, p = 0.009, n = 11) and at 16 h (r = +0.875, p = 0.022, n = 6) (Figure 5).

The analysis between the left superior cervical ganglion and the left or right retinas demonstrated significant positive correlations versus the right retina at 07 h (r = +0.806, p = 0.002, n = 11) and 01 h (r = +0.783, p = 0.021, n = 8). The analysis between the right superior cervical ganglion and the left or right retinas demonstrated significant positive correlations versus the right retina at 07 h (r = +0.726, p = 0.011, n = 11) and also, positive versus the left retina at 22 h (r = +0.875, p = 0.022, n = 6). The analysis between the left occipital cortex and the left or right retinas demonstrated significant positive correlations versus the right retina at 07 h (r = +0.733, p = 0.01, n = 11), versus the left retina at 13 h (r = +0.816, p = 0.047, n = 6), versus the right retina at 01 h (r = +0.841, p = 0.009, n = 8), and versus the right retina at 04 h (r = +0.921, p = 0.001, n = 8). The analysis between the right occipital cortex and the left or right retinas demonstrated significant positive correlations versus the right retina at 07 h (r = +0.792, p = 0.003, n = 11), versus the left (r = +0.799, p = 0.017, n = 8) and right (r = +0.763, p = 0.027, n = 8) retinas at 10 h, versus the left (r = +0.964, p = 0.001, n = 6) and right (r = +0.877, p = 0.021, n = 6) retinas at 22 h, and versus the left retina at 01 h (r = +0.754, p = 0.03, n = 8) (Figure 6).

The analysis between the anterior pituitary and the left or right retinas demonstrated a positive correlation that was close to significant versus the left retina at 07 h (r = +0.598, p = 0.052, n = 11) and a significant positive correlation versus the right retina (r = +0.747, p = 0.008, n = 11), a significant positive correlation versus the left (r = +0.933, p = 0.006, n = 6) and right (r = +0.832, p = 0.04, n = 6) at 22 h, and a significant positive correlation versus the right retina at 01 h (r = +0.921, p = 0.001, n = 8). The analysis between the posterior pituitary and the left or right retinas demonstrated a significant positive correlation with the left retina (r = +0.609, p = 0.046, n = 11) and also, a positive correlation with the right retina (r = +0.668, p = 0.024, n = 11) at 07 h (Figure 7).

The analysis between the pineal gland and the left or right retinas demonstrated a significant positive correlation versus the left retina (r = +0.892, p = 0.016, n = 6) at 22 h. The analysis between the serum and the left or right retinas demonstrated a significant positive correlation versus the right retina (r = +0.720, p = 0.044, n = 8) at 04 h (Figure 8).

The correlational analysis between the left and right retinas demonstrated significant positive values at 10 h (r = +0.772, p = 0.024, n = 8), 13 h (r = +0.873, p = 0.023, n = 6), and 22 h (r = +0.852, p = 0.031, n = 6). The analysis between the left and right anterior hypothalamus demonstrated significant positive correlations at 07 h (r = +0.930, $p < 0.0001$, n = 11), 13 h (r = +0.967, p = 0.001, n = 6), and 01 h (r = +0.871, p = 0.004, n = 8). The analysis between the left and right posterior hypothalamus demonstrated significant positive correlations at 07 h (r = +0.929, $p < 0.0001$, n = 11), 10 h (r = +0.801, p = 0.016, n = 8), 16 h (r = +0.948, p = 0.004,

$n = 6$), 22 h ($r = +0.981$, $p = 0.0005$, $n = 6$), and 01 h. ($r = +0.955$, $p = 0.0002$, $n = 8$) and a significant negative correlation at 13 h ($r = -0.820$, $p = 0.045$, $n = 6$). The analysis between the left and right superior cervical ganglion demonstrated significant positive correlations at 07 h ($r = +0.924$, $p < 0.0001$, $n = 11$), 13 h ($r = +0.900$, $p = 0.014$, $n = 6$), 01 h ($r = +0.766$, $p = 0.026$, $n = 8$), and 04 h ($r = +0.712$, $p = 0.047$, $n = 8$). The analysis between the left and right occipital cortex demonstrated significant positive correlations at 07 h ($r = +0.934$, $p < 0.0001$, $n = 11$), 10 h ($r = +0.710$, $p = 0.048$, $n = 8$), and 22 h ($r = +0.840$, $p = 0.036$, $n = 6$) (Figure 9).

4. Discussion

In the present study we attempted to analyze the diurnal behavior of the correlation levels of pGluPI activity between different photoneuroendocrine locations in adult male rats under a 12 h light/12 h dark cycle. We studied the diurnal pattern of correlation of pGluPI activity between the left (ReL) and right (ReR) retina, as well as the diurnal patterns of correlations between the rest of locations versus ReL or ReR. At this point, although the present analysis aimed to obtain new correlational data from previously reported results [5], it is necessary to acknowledge some limitations in the initial approach, to support possible future research. Firstly, we should note the small number of animals that we were able to use for some time points (it is necessary to take into account that for a correlational study between ReL or ReR and the rest of the locations, the data have to be paired) and secondly, for a more complete view of the cyclic behavior of the activity, it would have been necessary to add an additional time point at 19 h, at the beginning of the dark period. The results showed a great diversity of profiles, with no clear diurnal pattern of correlations between the different locations, and no similarity with the diurnal profile between ReL and ReR (Figures 4–8). The diurnal profiles also differed in the correlations between the left and right sides of the paired structures analyzed (Figure 9). Furthermore, there was usually no parallel between the diurnal profiles of the different correlation levels and the profile that showed the corresponding mean activity levels. If we analyze the levels of hydrolytic activity between two experimental groups, we may observe an increase in this activity in one of them, which would indicate the lower function of its substrate. In other words, although the levels of the substrate may increase, its function could be inhibited due to the high levels of the enzyme that inactivates or metabolizes it, and vice versa, if we observe lower levels of activity. On the other hand, the correlation levels reflect the possible intensity of interaction between two locations: a possible dependence (positive or negative correlation) or independence (no correlation). Therefore, correlational study offers a different perspective, not necessarily analogous to the studies of levels of enzymatic activity.

In the retina (Figure 4), the correlation levels between the ReL and ReR were positive, increasing at 10 h and 13 h and decreasing at 16 h in the light period, then increasing at 22 h in the dark period and slightly decreasing at 01 h and 04 h in the dark period, always with a positive character. Regarding the profile of the mean values, after a slight decrease compared with the levels at 07 h, the mean levels of the ReL and ReR showed profiles similar to those of the correlations. However, the inverse asymmetry observed with left predominance at 10 h and right predominance at 01 h does not seem to be related to the correlation levels because, although there was a significant level at 10 h, at the other hours when the correlation levels were significant (13 h and 22 h), no asymmetry was observed. However, there was asymmetry at 01 h, when the correlation was not significant.

Figure 5 shows the correlation levels between the ReL or ReR and the left anterior hypothalamus, right anterior hypothalamus, left posterior hypothalamus, and right posterior hypothalamus. Except for some generally negative correlation levels in the dark period compared with generally positive correlation levels in the light period, the profiles differed from one location to another. The correlation profiles did not resemble those of the mean values either. The posterior hypothalamus showed particularly remarkable behavior; except for a slight decrease in the positive correlation between the left posterior

hypothalamus and the left retina, the level of positive correlation between the PHtL versus the ReL or ReR remained stable between 07 h and 22 h. However, after 22 h, the correlation changed to negative, becoming significant for PHtL vs. ReL. Unlike PHtL, although the correlation profile was similar at 07 h, 10 h, 16 h, 22 h, 01 h, and 04 h, at 13 h, the correlations were negative both between the PHtR versus ReL and between the PHtR versus ReR. This differential behavior between the correlations of the left and right posterior hypothalamus versus the left and right retinas at 13 h could be related to the surprising asymmetric behavior of the correlation of the left versus right posterior hypothalamus at 13 h (Figure 9). Unlike the other time points when there were high levels of positive correlation, there was a high negative correlation at 13h: the greater the activity in the right posterior hypothalamus, the lower the activity in the left. The profile of the correlational behavior of the posterior hypothalamus differed from the profile observed in the mean values, in which there was a clear increase in activity in the left and right posterior hypothalamus at 13 h. We can rule out the suggestion that the correlational behavior at 13 h was incorrect, because the average of the individual values at 13 h indicated homogeneous levels of activity, with low SEM and, in addition, the result of the correlation between retinas and left posterior hypothalamus was different from the result of the correlation between retinas and right posterior hypothalamus.

Figure 6 shows the diurnal levels of correlation between the ReL or ReR and the left superior cervical ganglion, right superior cervical ganglion, left occipital cortex, and right occipital cortex. The profiles of the left and right superior cervical ganglia appeared inverse when comparing the correlations versus ReL and ReR and also differed from the previous profiles of the retina (Figure 4) and hypothalamus (Figure 5). Furthermore, they did not resemble the diurnal profiles of the mean values ± SEM for either structure.

Figure 7 shows the diurnal levels of correlation between the ReL or ReR and the anterior or posterior pituitary. The behavior of both did not seem to resemble any of the above nor did it offer a parallel with the mean values.

Figure 8 shows the diurnal levels of correlation between the ReL or ReR and the pineal gland and serum. The behavior at both locations also indicates the heterogeneity of diurnal profiles in the photoneuroendocrine circuit that we analyzed.

Figure 9 shows the diurnal correlation profiles between the left and right sides of the paired structures that we analyzed. It is interesting to note that high levels of negative correlation were only observed between the left and right sides of the posterior hypothalamus at 13 h during the light period, which coincided with high mean levels in both sides of the posterior hypothalamus at the same time. The rest of the analyzed time points in the light and dark periods showed highly significant levels of positive correlation between the left and right sides of the posterior hypothalamus. The dissection of the posterior hypothalamus that we obtained included, among other things, the arcuate nucleus [14]. The arcuate nucleus is essential in the control of energy homeostasis [16]. This nucleus receives excitatory and inhibitory projections from the suprachiasmatic nucleus, which has direct information about light and darkness from the retina and is considered the generator of biological rhythms [17]. The period of activity in the rat, with high energy homeostasis, is the nocturnal one and there is a low level of activity during daylight hours [18]. Thyrotropin-releasing hormone (TRH), a substrate of pGluPI [1], has an essential role in energy metabolism [19] and the arcuate nucleus, which contains TRH, is involved in a transient anorexigenic effect [20]. However, in addition to the presence of TRH in the posterior hypothalamus, we must take into account possible interaction with other multiple neurotransmitters involved in energy metabolism, such as histamine [21,22] or orexins [23]. We cannot forget the presence of melatonin receptors in the arcuate nucleus and their participation in the regulation of energy homeostasis [24–26]. According to all the above, with the present results obtained in the posterior hypothalamus, we could speculate on low energy metabolism towards the middle of the light period (13 h) related to a high level of negative correlation between the PHtL versus the PHtR.

It is interesting to remark that the correlation of the right posterior hypothalamus versus the left and right retinas also showed negative values at 13 h, which might implicate the right posterior hypothalamus (rather than the left) in the negative correlation behavior between both sides of the posterior hypothalamus (Figure 10). While the left retina had a negative correlation with the right posterior hypothalamus and a positive correlation with the left, the right retina had a negative correlation with the right posterior hypothalamus and a positive correlation with the left, or in other words, the right posterior hypothalamus correlated negatively with the left and right retinas and the left posterior hypothalamus positively with both. Furthermore, except for the unpaired locations APt and PPt, which correlated significantly at 07 h with both ReL and ReR, and Pi and S, which did not correlate significantly with any retina, most of the paired locations (AHtL, AHtR, PHtR, SCGL, SCGR, OCL, and OCR) correlated significantly with ReR only at 07 h, at the beginning of the light period, except PHtL, which correlated significantly only with ReL. This is also interesting because it highlights the existence of a diurnal functional asymmetry dependent on the ambient light and darkness.

Using other different and specific nonstandard light–dark schedules, Sanchez et al. [27] concluded that light and darkness clearly influenced pGluPI activity under the specific conditions of their experiment; light increased activity in the ReL and darkness increased it in the ReR. In the anterior hypothalamus, while no asymmetry was observed with light, there was a left predominance with darkness. In the present research, the lack of data at the beginning of the dark period (19 h) does not allow us to reach such a specific conclusion. In addition, other studies with nonstandard light–dark schedules, such as constant light or darkness conditions [28], demonstrated that the regional pattern of distribution of pGluPI activity in locations of the photoneuroendocrine circuit was similar in groups under a standard light–dark schedule and in groups tested under constant light or dark conditions. However, this pattern differed between groups subjected to the standard versus the constant light–dark conditions. Those results also suggest an influence of environmental light and darkness on pGluPI activity, which may reflect concomitant changes in its susceptible substrates and consequently, in their functions. It would be interesting to analyze the left versus right correlational behavior under these nonstandard specific conditions. More recent studies with other proteolytic enzymes, such as alanyl aminopeptidase (EC 3.4.11.2), in left and right retina under standard and nonstandard (constant light) conditions, have also demonstrated important asymmetrical differences between the groups studied. This suggests that other substrates, in this case, enkephalins among others, also respond asymmetrically to environmental conditions and that the functional response depends on the interaction of the various involved factors [29].

5. Conclusions

The diurnal correlation profiles between the various locations analyzed versus the left or right retinas showed great diversity without a clear defined pattern, and they showed asymmetric behavior in terms of their correlations with the ReL and ReR. Also, the pattern of the correlation levels did not correspond to that of the mean activity levels. The correlation between the left and right sides of the paired structures showed high positive levels except at 13 h during the light period, when a high level of negative correlation between the left and right posterior hypothalamus was observed. This result seems to stand out from the rest and draws our attention to the asymmetric behavior of the posterior hypothalamus towards the middle of the light period, in which the rats showed low levels of energy homeostasis. In addition, except for the posterior hypothalamus, the majority of the paired locations correlated significantly with the right retina only at 07 h of the light period. In general terms, these results demonstrate the complexity of the study of brain asymmetry and allow us to conclude, as we previously indicated [30], that it is a dynamic process dependent on multiple exogenous and endogenous factors that condition the physiology of the animal.

Author Contributions: Conceptualization, M.R.-S.; writing—original draft preparation, M.R.-S.; writing—review and editing, M.R.-S., I.P., A.B.S., I.B., M.M.-C., G.D.-V., R.D. and F.V.; funding acquisition, M.R.-S., I.P., A.B.S. and I.B. All authors have read and agreed to the published version of the manuscript.

Funding: This research was supported by the group of the University of Jaén "Neuroendocrinology and Nutrition" BIO-221.

Data Availability Statement: The data presented in this study are available on request from the corresponding author.

Conflicts of Interest: The authors declare no conflicts of interest.

References

1. O'Cuinn, G.; O'Connor, B.; Elmore, M. Degradation of thyrotropin-releasing hormone and luteinising hormone-releasing hormone by enzymes of brain tissue. *J. Neurochem.* **1990**, *54*, 1–13. [CrossRef] [PubMed]
2. Brunetti, L.; Cacciatore, I.; Di Stefano, A.; Duprè, S.; Giorgi, A.; Luisi, G.; Michelotto, B.; Orlando, G.; Pinnen, F.; Recinella, L.; et al. Synthesis and biological evaluation of a novel pyroglutamyl-modified TRH analogue. *Farmaco* **2002**, *57*, 479–486. [CrossRef]
3. Alba, F.; Arenas, J.C.; Lopez, M.A. Comparison of soluble and membrane-bound pyroglutamyl peptidase I activities in rat brain tissues in the presence of detergents. *Neuropeptides* **1995**, *29*, 103–107. [CrossRef]
4. Jiang, H.; Gong, Q.; Zhang, R. Pyroglutamyl aminopeptidase 1 is a potential molecular target toward diagnosing and treating inflammation. *Front. Immunol.* **2023**, *14*, 1301539. [CrossRef] [PubMed]
5. Ramirez, M.; Sanchez, B.; Arechaga, G.; Garcia, S.; Lardelli, P.; Venzon, D.; de Gandarias, J.M. Diurnal variation and left-right distribution of pyroglutamyl peptidase I activity in the rat brain and retina. *Acta Endocrinol.* **1991**, *125*, 570–573. [CrossRef]
6. Teclemariam-Mesbah, R.; Ter Horst, G.J.; Postema, F.; Wortel, J.; Buijs, R.M. Anatomical demonstration of the suprachiasmatic nucleus-pineal pathway. *J. Comp. Neurol.* **1999**, *406*, 171–182. [CrossRef]
7. Korf, H.W.; Oksche, A.; Ekström, P.; Gery, I.; Zigler, J.S., Jr.; Klein, D.C. Pinealocyte projections into the mammalian brain revealed with S-antigen antiserum. *Science* **1986**, *231*, 735–737. [CrossRef] [PubMed]
8. Saeb-Parsy, K.; Lombardelli, S.; Khan, F.Z.; McDowall, K.; Au-Yong, I.T.; Dyball, R.E. Neural connections of hypothalamic neuroendocrine nuclei in the rat. *J. Neuroendocrinol.* **2000**, *12*, 635–648. [CrossRef] [PubMed]
9. Youngstrom, T.G.; Weiss, M.L.; Nunez, A.A. Retinofugal projections to the hypothalamus, anterior thalamus and basal forebrain in hamsters. *Brain Res. Bull.* **1991**, *26*, 403–411. [CrossRef]
10. Cusick, C.G.; Lund, R.D. The distribution of the callosal projection to the occipital visual cortex in rats and mice. *Brain Res.* **1981**, *214*, 239–259. [CrossRef]
11. Klosen, P. Thirty-seven years of MT1 and MT2 melatonin receptor localization in the brain: Past and future challenges. *J. Pineal Res.* **2024**, *76*, e12955. [CrossRef] [PubMed]
12. Felder-Schmittbuhl, M.P.; Hicks, D.; Ribelayga, C.P.; Tosini, G. Melatonin in the mammalian retina: Synthesis, mechanisms of action and neuroprotection. *J. Pineal Res.* **2024**, *76*, e12951. [CrossRef] [PubMed]
13. Ramírez, M.; Prieto, I.; Banegas, I.; Segarra, A.B.; Alba, F. Neuropeptidases. *Methods Mol. Biol.* **2011**, *789*, 287–294. [PubMed]
14. Konig, J.F.R.; Klippel, R.A. *The Rat Brain*; Krieger: Huntington, NY, USA, 1967.
15. Bradford, M.M. A rapid and sensitive method for the quantitation of microgram quantities of protein utilizing the principle of protein-dye binding. *Anal. Biochem.* **1976**, *72*, 248–254. [CrossRef] [PubMed]
16. Kuczynski-Noyau, L.; Karmann, S.; Alberton, P.; Martinez-Corral, I.; Nampoothiri, S.; Sauvé, F.; Lhomme, T.; Quarta, C.; Apte, S.S.; Bouret, S.; et al. A plastic aggrecan barrier modulated by peripheral energy state gates metabolic signal access to arcuate neurons. *Nat. Commun.* **2024**, *15*, 6701. [CrossRef]
17. Saeb-Parsy, K.; Dyball, R.E. Defined cell groups in the rat suprachiasmatic nucleus have different day/night rhythms of single-unit activity in vivo. *J. Biol. Rhythms* **2003**, *18*, 26–42. [CrossRef]
18. Page, A.J.; Christie, S.; Symonds, E.; Li, H. Circadian regulation of appetite and time restricted feeding. *Physiol. Behav.* **2020**, *220*, 112873. [CrossRef]
19. Lechan, R.M.; Fekete, C. The TRH neuron: A hypothalamic integrator of energy metabolism. *Prog. Brain Res.* **2006**, *153*, 209–235.
20. Vargas, Y.; Castro Tron, A.E.; Rodríguez Rodríguez, A.; Uribe, R.M.; Joseph-Bravo, P.; Charli, J.L. Thyrotropin-Releasing Hormone and Food Intake in Mammals: An Update. *Metabolites* **2024**, *14*, 302. [CrossRef]
21. Umehara, H.; Mizuguchi, H.; Fukui, H. Identification of a histaminergic circuit in the caudal hypothalamus: An evidence for functional heterogeneity of histaminergic neurons. *Neurochem. Int.* **2012**, *61*, 942–947. [CrossRef]
22. Monti, J.M. Involvement of histamine in the control of the waking state. *Life Sci.* **1993**, *53*, 1331–1338. [CrossRef] [PubMed]
23. Yoshida, K.; McCormack, S.; España, R.A.; Crocker, A.; Scammell, T.E. Afferents to the orexin neurons of the rat brain. *J. Comp. Neurol.* **2006**, *494*, 845–861. [CrossRef] [PubMed]
24. Drew, J.E.; Barrett, P.; Mercer, J.G.; Moar, K.M.; Canet, E.; Delagrange, P.; Morgan, P.J. Localization of the melatonin-related receptor in the rodent brain and peripheral tissues. *J. Neuroendocrinol.* **2001**, *13*, 453–458. [CrossRef] [PubMed]

25. Williams, L.M.; Hannah, L.T.; Hastings, M.H.; Maywood, E.S. Melatonin receptors in the rat brain and pituitary. *J. Pineal Res.* **1995**, *19*, 173–177. [CrossRef] [PubMed]
26. Buonfiglio, D.; Tchio, C.; Furigo, I.; Donato, J., Jr.; Baba, K.; Cipolla-Neto, J.; Tosini, G. Removing melatonin receptor type 1 signaling leads to selective leptin resistance in the arcuate nucleus. *J. Pineal Res.* **2019**, *67*, e12580. [CrossRef]
27. Sánchez, B.; Alba, F.; Luna, J.D.; Martínez, J.M.; Prieto, I.; Ramírez, M. Pyroglutamyl peptidase I levels and their left-right distribution in the rat retina and hypothalamus are influenced by light-dark conditions. *Brain Res.* **1996**, *731*, 254–257. [CrossRef]
28. Ramírez, M.; Arechaga, G.; Martínez, J.M.; Prieto, I.; Ramírez-Expósito, M.J.; Sánchez, B.; Alba, F. Environmental light-darkness conditions induce changes in brain and peripheral pyroglutamyl-peptidase I activity. *Neurochem. Res.* **2001**, *26*, 463–468. [CrossRef]
29. Domínguez-Vías, G.; Aretxaga, G.; Prieto, I.; Segarra, A.B.; Luna, J.D.; Martínez-Cañamero, M.; Ramírez-Sánchez, M. Asymmetrical influence of a standard light/dark cycle and constant light conditions on the alanyl-aminopeptidase activity of the left and right retinas in adult male rats. *Exp. Eye Res.* **2020**, *198*, 108149. [CrossRef]
30. Ramírez-Sánchez, M.; Prieto, I.; Segarra, A.B.; Banegas, I.; Martínez-Cañamero, M.; Domínguez-Vías, G.; de Gasparo, M. Brain Asymmetry: Towards an Asymmetrical Neurovisceral Integration. *Symmetry* **2021**, *13*, 2409. [CrossRef]